Micro-Fabrication and Operation Nano Emitters Suitable for a Colloid Thruster Array

John Stark[1] Bob Stevens[2] Barry Kent[2] Mike Sandford[2] and Matthew Alexander[1]
[1]Department of Engineering, Queen Mary, University of London UK
[2] Central Microstructures Facility, Rutherford Appleton Laboratory, UK

Abstract

The current interest in colloid propulsion has been stimulated in part by the opportunity afforded by micro-fabrication techniques to produce multi-element arrays of capillary emitters, each one of which supports a single Taylor cone structure, and produces a spray of charged droplets. The low flow rate necessitated for stable cone-jet mode electrospray, identifies the need for a significant number of individual emitters if a sufficient level of thrust is to be obtained, to make such devices applicable to space missions. This integrated, micro-fabricated colloid thruster requires a number of key components including not only the emitter array, but also a propellant feed system, a propellant reservoir, and either one or two electrostatic grids to establish the electrospray process and subsequently accelerate the charged droplets to an appropriate velocity. As a first step in the realization of an integrated micro-technology colloid thruster, the fabrication of a range of nano-emitters has been achieved, permitting a high emitter density to be obtained. Such arrays may be used to provide a relatively high thrust density from a colloid thruster, typically of order 100N/m^2. In this paper the nano-emitter fabrication processes are described and electrospray properties from individual nano-emitters are presented.

Colloid Thruster Concepts

The key elements of a colloid thruster are shown schematically in figure 1. An emitter, most frequently in the form of a capillary is used to supply a conductive fluid into a region of an intense electric field, typically of order 10^5 to 10^6 V/m. As observed originally by Zeleny [1] and subsequently characterized by Taylor [2] a balance between fluidic forces associated with surface tension and any applied static pressure, with the electric stress exerted on the fluid, results in a stable 'Taylor'- cone. Increased electric stress results in the formation of a stable jet, under certain conditions, which eventually breaks up into a stream of charged droplets. These droplets are accelerated in the electric field in order to produce thrust. A fluid is stored in a reservoir, or propellant tank, which supplies fluid to the emitter. As in all electrostatic thrust devices the charged beam is required to be electrically neutral and some method is required to supply oppositely charged species into the plume. Most concepts result in a positive charge on the droplets, requiring electron injection to the plume to achieve neutralization. It has been noted however by Perel [3] that the electrospray process operates in like manner independently of the relative field direction between the emitter and grid, with a positive emitter potential relative to an 'accelerator' electrode yielding a positive droplet, whilst a negative potential reverses the droplet charge. Thus in a colloid thruster it may be possible to remove the need for a neutralizer by having multiple emitters, some of which are positive and some negative.

Differing thruster concepts arise from the way in which these key components are utilized and realized. Historically all development focused upon the use of

individual capillary structures fabricated into an array, with discrete components used for propellant storage, supply and control, accelerator grid(s) and neutralization. Additionally the size of the capillary used in older concepts tended to be rather large, and not necessarily linked to the anticipated flow rate through the emitter.

Currently there is a resurgence of interest in colloid propulsion systems, although still most of the published results from this work focus upon data from configurations with discrete elements in the thruster. Thus collaborative work reported from MIT [4] in association with Yale and Busek [5], has led to the development of a thruster, which contains 57 individual stainless steel emitters brazed into a supporting structure. These emitters are quite long, 1cm, and have an internal diameter of 30 μm. The propellant is highly doped formamide, with a conductivity of 0.5S/m. The work at Stanford has a larger array of 100 hypodermic needles, with doped glycerol as the propellant [6].

Previous examples of micro-fabricated emitters include those obtained for use in mass spectrometry. Capillary structures were fabricated in the wafer plan; they had tapered tips with a 5μm by 10μm exit profile [7]. Several hours of electrospraying was achieved by applying a few kV to a close-by but separate, macro-scale electrode. Another group [8] etched 10μm diameter nozzles through the thickness of a silicon wafer; they stand 50μm above the surface. Sprays were obtained when 1250V was applied to the nearby mass spectrometer sampling cone. These examples however relate to the nano-electrospray mode whereby it is the electrostatic stress on the fluid, which extracts the fluid, as there is no positive pressure applied.

In this paper we focus upon the fabrication processes for silicon nano-emitters, with application to colloid thrusters. Both arrays of nozzles and individual nozzle emitters have been fabricated, and we compare electrospray properties from these emitters with those sprays formed from conventional emitters.

Nano-Emitter Fabrication Processes.

The fabrication sequence described facilitates manufacture of single nozzle and wafer-level multiple nozzle arrays. The starting material was 100mm diameter, 1 mm thick N-type 1-10 Ohm-cm, double side polished silicon wafers. The first step was to deposit silicon dioxide on to both sides (Sides 1 and 2) by wet thermal oxidation. An additional 2 μm layer of silicon dioxide was deposited on side 1 of the wafer by Plasma Enhanced Chemical Vapour deposition.

Following Hexamethyldisilizane (HMDS) treatment of side 1, side 1 was coated with 10μm of AZ4562 photoresist, by dispensing 250μl of AZ4562 into the centre of the wafer and then spin coating at 1400 rpm for 28 seconds, with an acceleration of 500 $rpm.s^{-1}$. The layer was baked for 10 minutes on a hotplate at 90C. Hard contact Ultra Violet (UV) exposure through a chrome on borosilicate glass mask was used to photodefine the AZ4562 resist. A Karl Suss MA6 aligner was used to centre the wafer with respect to the lithographic mask. The broad band UV dose was generated by a high pressure mercury vapour lamp, and the dose conditions were an exposure time of 25 seconds with an illumination intensity of 10 $mWcm^{-2}$. The exposed photoresist layer was then developed in a tank of aqueous developer solution, which consisted of four parts de-ionised with one part AZ400K developer, by volume. The develop time was 5 minutes which ensured that all the exposed resist was removed. The layer was then rinsed in a weir wash with de-ionised water for 3 minutes and then spin dried under a nitrogen gas stream at 2000 rpm for 80 seconds. The wafer was subjected to an oxygen plasma descum, for 2 minutes using a parallel plate reactive ion etching systems, (Oxford Plasma Technology ,RIE80 plus). The process conditions were an RF power

of 300 W at a pressure of 100 mTorr, and an oxygen flow rate of 100sccm.

After descum, the wafers were loaded into a parallel plate reactive ion etch system. The 6um of silicon dioxide was etched using an Argon (Ar) (7sccm) and CHF3 (21 sccm) plasma at 250W and a pressure of 30mTorr. The etch time was 6 hours. The remaining AZ4562 resist layer was ashed in an oxygen plasma. The etched oxide surface was then protected from possible surface damage by spin coating PI 2771 polyimide from HD microsystems and baking at 300C for 30 minutes on a hotplate. The oxide layer on side 2 was then prepared for patterning by an aggressive oxygen plasma clean and then deposition of HMDS. The process steps described above were used to define the oxide etch mask on side 2. The resulting cross-section is shown in figure 2.

After oxide mask definition the wafer was immersed in EKC265 for 1 hour at 70C to remove all organic layers from sides 1 and 2. The wafer was then rinsed and dried. A 100mm diameter silicon carrier wafer was then coated with 'Cool Grease' which has high thermal conductivity. Side 2 of the device wafer is then bonded to the greased surface of the carrier wafer by placing on a hotplate at 90C for 5 minutes. Side 1 of the wafer sandwich is descummed in an oxygen plasma and then a photoresist layer of AZ4562 is coated and the aligned in-contact mask is defined by standard photolithographic techniques described earlier. The descummed surface is than loaded into a Surface Technology Systems Inductively Coupled Plasma Reactive Ion etcher with the capability to run an Advanced Silicon Etch (ASE), which uses SF6 as the silicon etch process and C4F8 as the passivation gas. The first process is to produce a 5 μm undercut of the in-contact mask, which enhances the aspect ratio of the subsequent anisotropic silicon DRIE etch which defines the 'through wafer' capillaries. The isotropic etch uses an ICP coil power of 500W with a platen power of 0W. The total etch time was 2.5 minutes. The capillary etch is then performed by using the cycling ASE process. There are two repeating cycles for the etch process. The etch cycle last for 12 seconds and uses SF6 at a flow rate of 135 sccm, with the automatic pressure controller in manual mode at 82%. The ICP coil was run at 800W and the platen power at 20W. Following the etch cycle the machine automatically switches to the passivation cycle. The passivation conditions were an ICP coil power of 600W and 0W platen power. for a time of 8 seconds. The total number of cyles was 720, which results in a etch depth of over 500μm. The etched wafer is then unloaded and the remaining resist layer removed by reactive ion etching. The wafer sandwich is then loaded into the ICP deep RIE where it is etched for 540 cycles to remove 400μm of silicon. This leaves a structure shown in figure 3. Following the etch to define the outside of the nozzle and to extend the depth of the nozzle capillary, the carrier wafer is debonded from the device wafer. Side 2 is cleaned using Iso Propyl Alchohol to remove the majority of the Cool Grease. The wafer is then immersed in EKC265 for 1 hour to remove any remaining organics. The wafer is rinsed and dried prior to loading into an Oxford Plasma Technology DP800 plasma enhanced chemical vapour deposition system. The process conditions were SiH4 (100sccm) and N2O(50sccm), platen temperature of 300C, RF power of 15W and a process time of 142 minutes. This deposits a conformal coating of silicon dioxide, which is 2μm thick, on side 1 of the wafer surface. The wafer is bonded to a new carrier wafer with side 1 facing the cool grease surface. The wafer is then descummed, prior to loading into the ICP deep RIE. A modified silicon etch process is used to expose the nozzle capillary as shown in figure 4. Then, after all capillaries have been uncovered, a photoresist is painted onto the etched recess to prevent further etching in the capillary regions. The DRIE is continued to etch through the wafer to define the 10mm diameter circular

die with single or multiple nozzle arrays. The die are then demounted from the carrier wafer using a vacuum pen and rinsed in IPA and EKC265. Following the removal of organic materials the die is place in a PTFE holder prior to oxide strip using 7:1 hydrofluoric acid. The resulting structure is shown in figure 5. The die are then rinsed and dried prior to mounting onto a stainless steel ring using a two part epoxy adhesive. The epoxy is cured in an oven at 90C for 1 hour. The assembly is loaded into DC magnetron sputtering system where a chromium thin film of 0.1μm is deposited followed by a copper layer of 2μm. The nozzle sub-assembly is shown in figure 6. Following this step the devices were assembled into the colloidal thruster test rig.

Nano-Emitter Fabrication Examples.

Figure 7 shows an SEM micrograph of the single silicon nozzle which was defined in the centre of a 10mm diameter silicon disk. The process allows single nozzles to be fabricated with minimum dimensions of 35μm outer diameter, with a 25μm diameter through hole and a height of 400μm.

The same process can produce clusters of nozzles, with a varying number of nozzles and pitch between nozzles. Figure 8 shows a 100mm diameter wafer with 55 electrospray heads. Each head has a cluster of nozzles at the centre of the 10mm diameter die. The number of nozzles per cluster range is either 3,7 or 19. The nozzle layout is in the form of triangular arrays. Figure 9 shows a plan view of a cluster with 7 nozzles.

A colloidal thruster required to provide a high thrust values may be realized by fabricating nano emitter arrays at the wafer scale. Figure 10 shows an example of a 100mm diameter wafer with 20,000 nozzles defined within the 75mm diameter central area. Figure 11 shows an SEM micrograph of this wafer. This demonstrates that uniform, repeatable multiple array nozzles can be defined using MEMs processes.

Finally, in figure 12 we show an array of three elements, each electrospraying a solution of ethylene glycol liquid, doped with NaI. This liquid has a conductivity of 0.01 S/m. It is notable that each of the 'Taylor cones' appears to have the same size and shape. The jet emitted from the cone is also visible. The slight divergence noted in this image is caused by the configuration of the counter electrode used in the test set-up.

Individual Nano-Emitter Electrospray Properties

The current voltage characteristics for a single nano-emitter micro-fabricated in silicon at four flow rates is shown in figure 13. The fluid used to obtain this data was tri-ethylene glycol, doped with NaI in order to achieve a conductivity of 0.01S/m. This emitter is coated in Cr/Cu, and has an external diameter of 400μm, internal diameter of 100μm. The emitter is 400μm long. This emitter was held in a specially manufactured holder. A high positive voltage was applied to a single grid, with a Faraday cup used to measure the spray current. Current monitoring on both the emitter and grid were also recorded within the vacuum configuration, as described in[5]. For the measurements displayed the grid was set at a distance of 4mm from the tip of the emitter. This data shows the general trend of an increasing gradient in the I:V curve, as the flow rate is increased; this is also noted in data from conventional capillary emitters [9].

Figure 14 is a plot of the current as a function of voltage at a single value of flow rate, 55 nl/s, again using the TEG solution having a conductivity of 0.01 S/m; here however we compare the emitter current for two different Si nano-emitters. One of these is the same emitter as used in the collection of data plotted in figure 12 - 400μm outside diameter, with 100μm internal diameter. The other emitter used has on outside

diameter of 560μm, with an internal diameter of 305μm. It is apparent that there is a significant difference in the current observed, with typically the current from the larger emitter being of order 50 to 60% greater. This variation between emitters is not predicted by scaling law models generally adopted to identify electrospray properties [10,11]; these generally neglect the detailed electrostatic and physical conditions of the capillary typically used in electrospray experiments. The increased current noted for the larger emitter is clearly suggestive that the increased area potentially available for oxidation reactions may influence the spray current. Indeed if such reactions only take place at the upper surface of the emitter, then it is interesting to observe the ratio of areas for these two emitters is 1.47. There are however other places where electrochemical reactions can occur, such as inside the relatively conductive inner bore, being high conductivity Si whose conductivity is in the range 1 –10 Ωcm. Clearly these results need further investigation: we have therefore fabricated a number of different emitter configurations and will be testing these to quantify further the effects of emitter geometry.

We have also attempted to compare the spray data obtained from the micro-fabricated emitters with data from a conventional capillary electrospray; this is plotted in figure 15. The data in this figure was obtained using the same fluid as before, and is shown for two flow rates: 55nl/s and 110nl/s. The emitter and capillary have the same values for internal and external diameters: 305μm and 560μm respectively, however the nano-emitter protrudes above the surrounding surface to only 400μm, whereas the capillary extends to 13mm above the surface on which it is mounted. This is the principal reason for the higher voltage required to achieve a stable electrospray in the case of the nano-emitter configuration. More detailed analysis of the electric field strength is presented in [12], however due to the changing cone shape structure with applied voltage, which is different for the nano emitter and the capillary, it has not been possible to compare directly the conditions between the capillary and nano-emitter electrospray properties. However the very similar magnitudes noted in the spray currents identifies that there appear to be no substantial influences in spray efficiency in these two specific examples investigated.

Conclusions

The fabrication of a range of nano-emitters has been achieved, which permits a high emitter density to be obtained. Such arrays may be used to provide a relatively high thrust density from a colloid thruster.

Comparison between spray properties from a nano emitter fabricated in silicon, and conventional stainless steel emitters has identified that there do not appear to be substantial differences in the spray current for capillaries and emitters that have the same internal and external diameters. We have observed however that for emitters having different values of internal and external diameters, that the spray current is different at the same flow conditions. These differences suggest that the geometric specification for a nano-emitter is important if high efficiency is to be achieved in a colloid thruster.

References

[1] Zeleny J., Phys Rev 10 1,(1917)
[2] Taylor GI, Proceedings Royal Society A280, 383 (1964)
[3] Perel, J , Bates T, Mahoney J, Moore RD, & Yahiku AY, AIAA paper 67-728, Colorado Springs, (1967)
[4] M Martinez-Sanchez, de la Mora,JF, HrubyV, Gamero Castano M V Khayms IEPC-99-014 (1999)
[5] Hruby V, Gamero-Castano M, Falkos P, Shenoy S, IEPC-01-281, (2001)
[6] IEPC paper no. 01-284, 27th IEPC, October 15-19, Pasadena, (2001)

[7] L. Licklider, X. Wang et al. "A micromachined Chip-based Electrospray Source for Mass Spectrometry", Anal Chem 72, pp 367-375, (2000)

[8] G. Schultz, T. Corso, S. Prosser, S. Zhang. "A Fully Integrated Monolithic Microchip Electrospray Device for Mass Spectrometry", Anal Chem 72, pp 4058-4063, (2000)

[9] Stark J, Smith K & Robertson S, to be presented 39th AIAA Joint Propulsion Conference (2003)

[10] Fernandez de la Mora J, & Loscertales JG, Journal Fluid Mechanics 260, 155 (1994)

[11] Ganan-Calvo AM, J Davila & A Barrero, J Aerosol Sci. 28, 249,(1997).

[12] Stark J , Kent B, Stevens R, Sandford M Alexander M and M Paine, to be presented 39th AIAA Joint Propulsion Conference (2003)

Figure 1

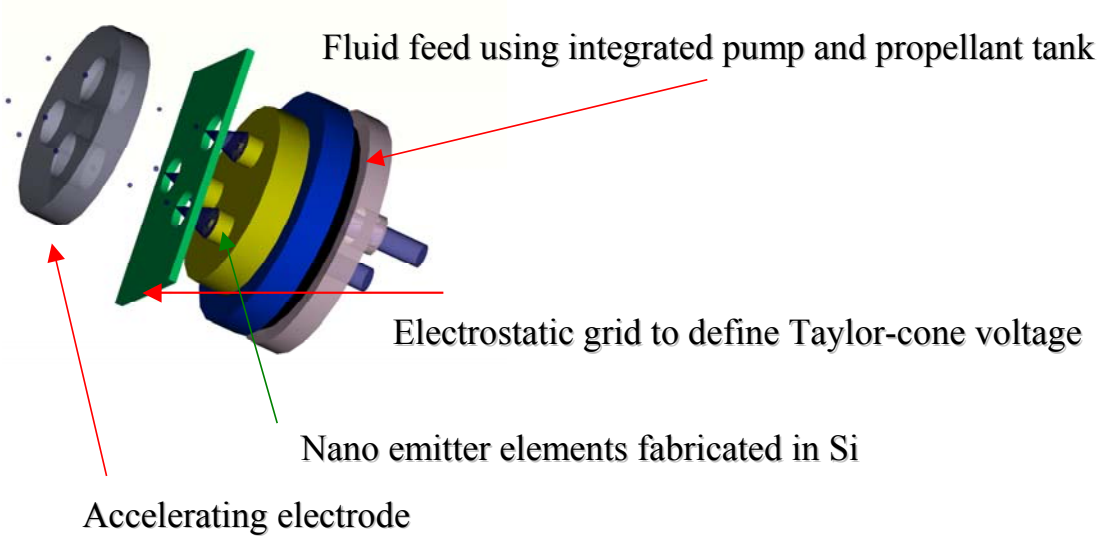

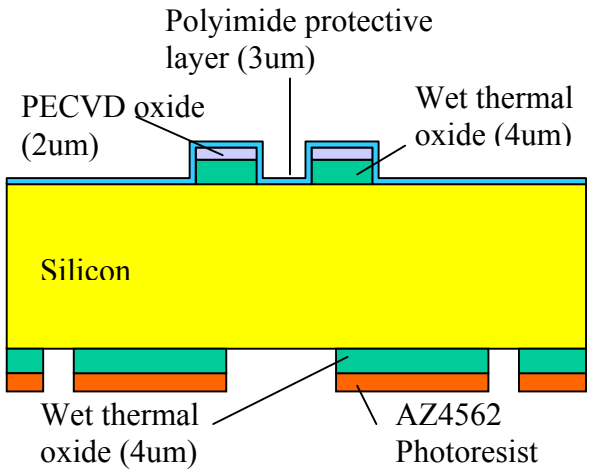

Figure 2

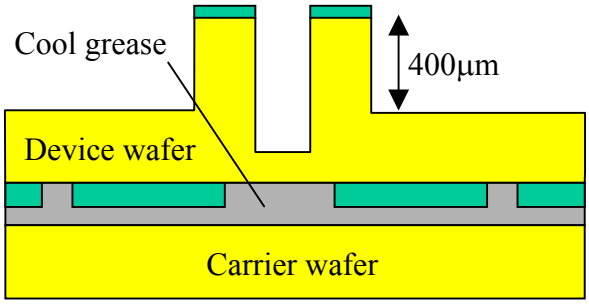

Figure 3

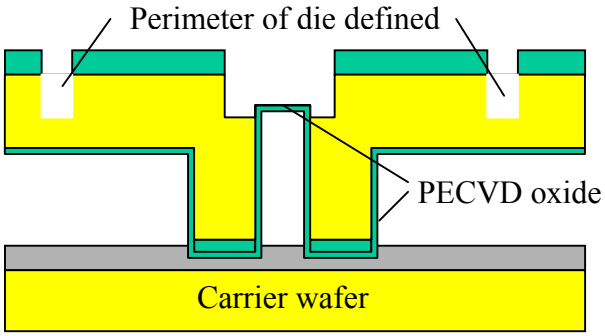

Figure 4

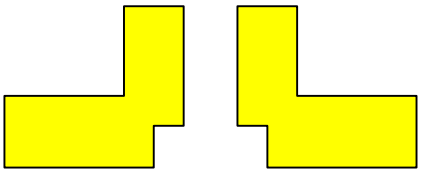

Silicon nozzle die after clean and oxide strip.

Figure 5

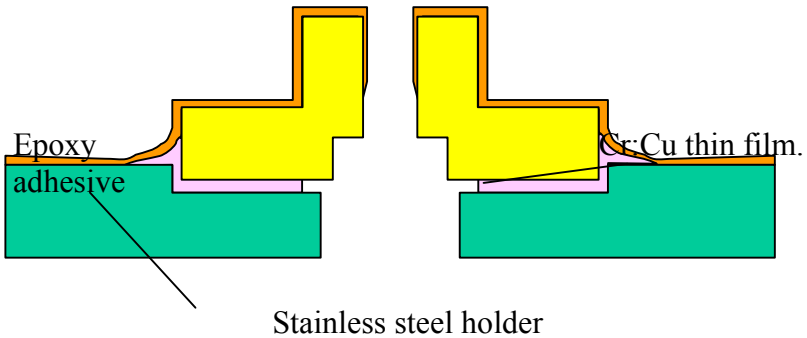

Figure 6

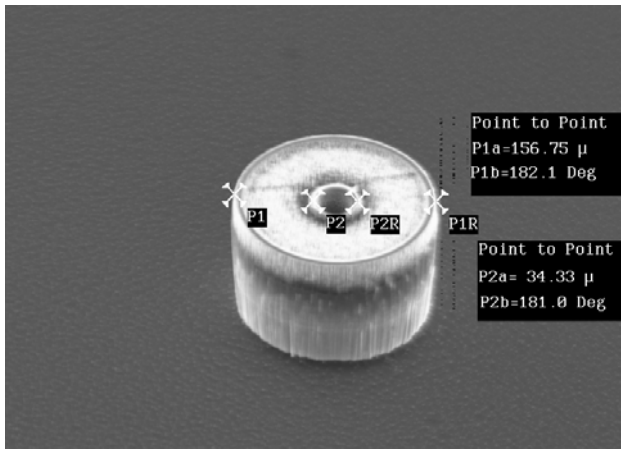

Single 150µm diameter electrospray nozzle.

Figure 7

Figure 8

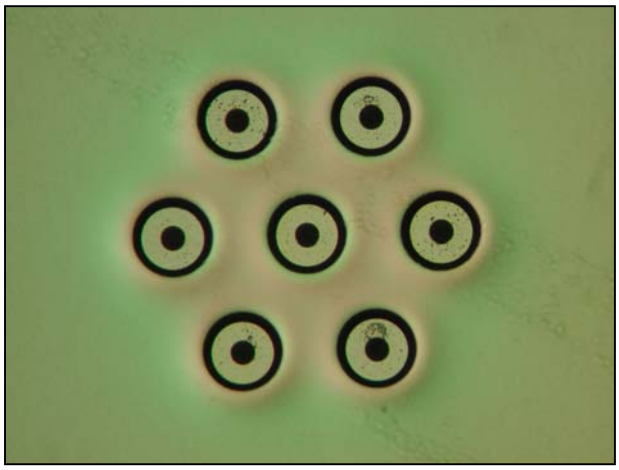

Figure 9

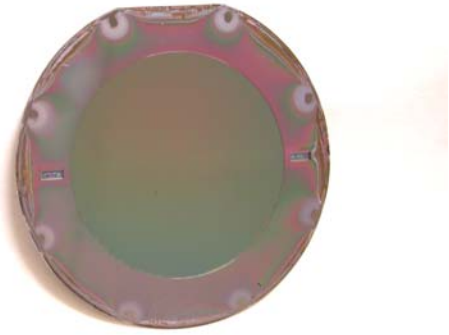

Colloidal Thruster nozzle wafer
with 20.000 silicon nozzles.

Figure 10

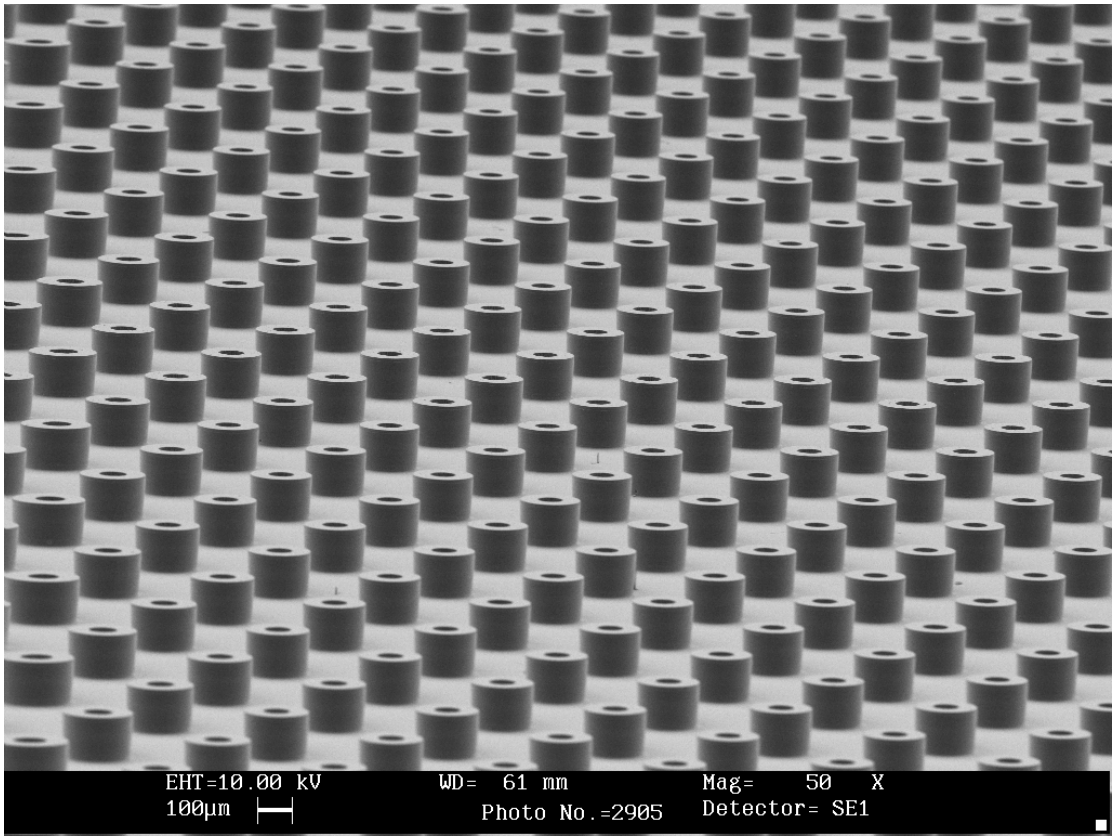

Figure 11

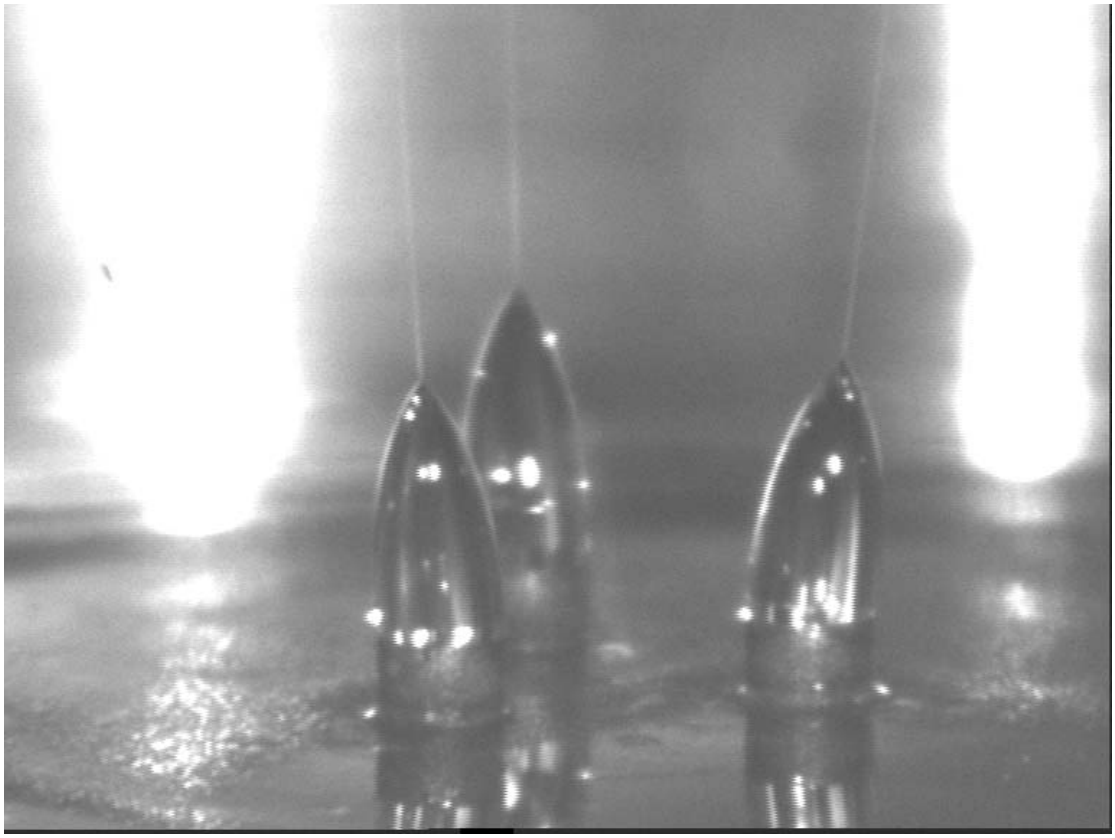

Figure 12 Electrospray from 3 nano-emitters

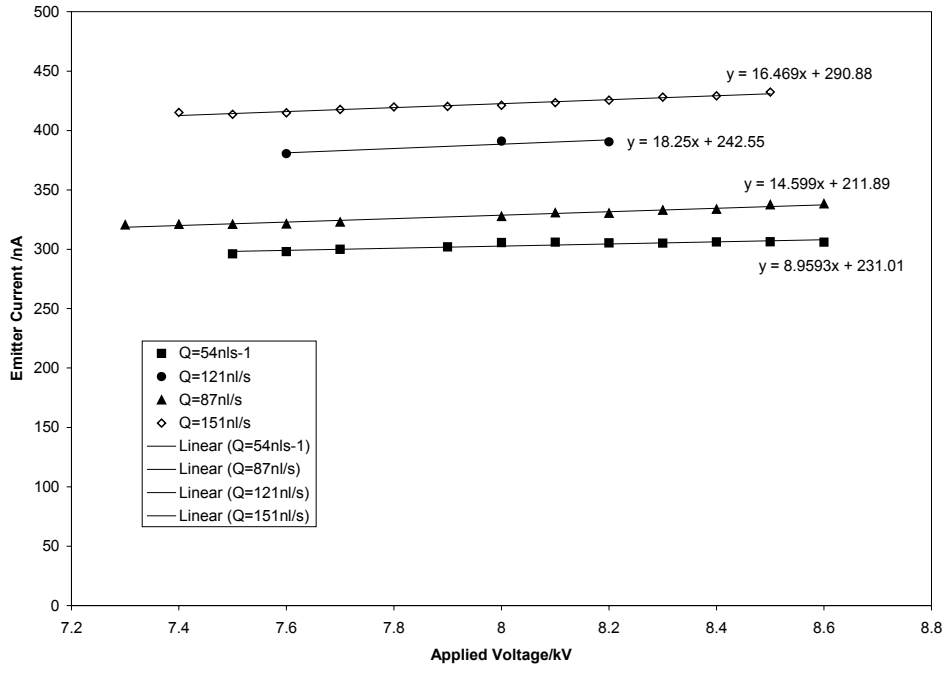

Figure 13 Electrospray I:V from single nano emitter

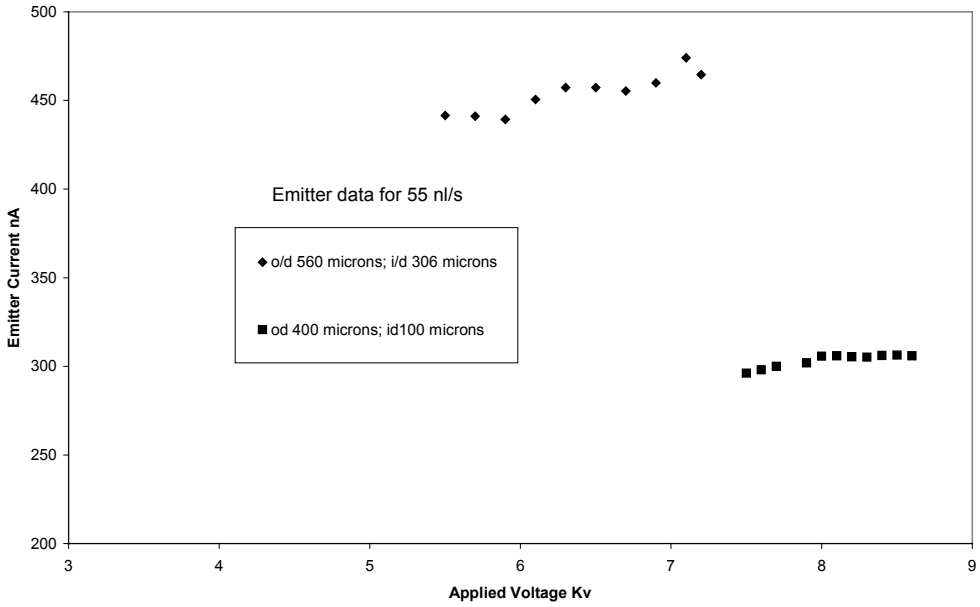

Figure 14 Comparison of spray current for Si nano-emitters with varying internal to external diameters at a flow rate of 55 nl/s.

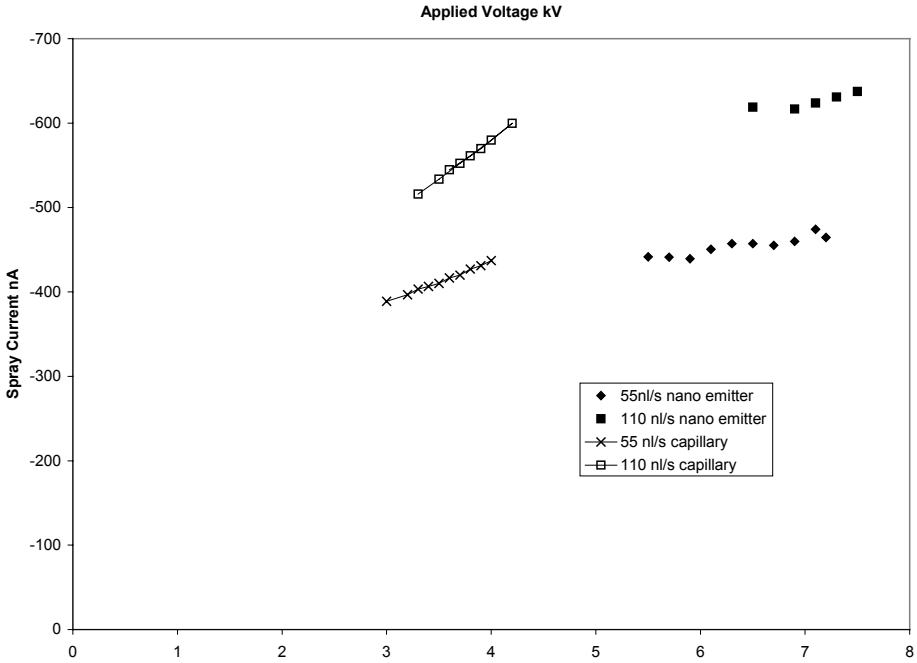

Figure 15 Comparison of spray currents from stainless steel capillary with silicon nano emitter having the same internal and external diameters; length of capillary 13 cm, length of nano emitter 400μm.